Purity monitoring for ProtoDUNE

Richie Diurba (University of Minnesota) for the DUNE Collaboration

ICHEP 2020

POSTER-20-070-LBNF

Liquid Argon Purity Monitoring

- Liquid argon time-projection-chambers (LAr TPCs) use drifted ionized electrons for calorimetry and tracking.
- Detector technology for neutrino experiments like DUNE and ICARUS. Even used for dark matter experiments like DarkSide.
- Electronegative impurities, like water and O_2, can capture ionized electrons and reduce the size of signals on the readout.
- ProtoDUNE operates a single-phase and dual-phase detector to prototype the eventual DUNE Far Detector modules.

Basics

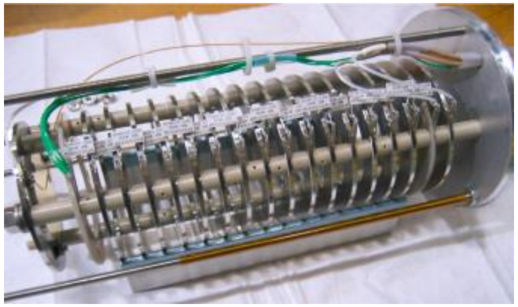

- ProtoDUNE utilizes purity monitors, the same design used for ICARUS, to quantify the LAr purity by measuring the lifetime of drift electrons [1].
- Uses a drift chamber that drifts electrons from a cathode to an anode.
- Stainless steel shaping rings guide the electrons.

Schematic of a Purity Monitor

- A flash from the Xe lamp leads to photoelectrons on the cathode.
- Electrons then drift in a 20 cm drift chamber in a high voltage typically between 250-500 V [1].
- Two Frisch grids in front of the anode and cathode sharpen the signal and shorten the signal's duration.

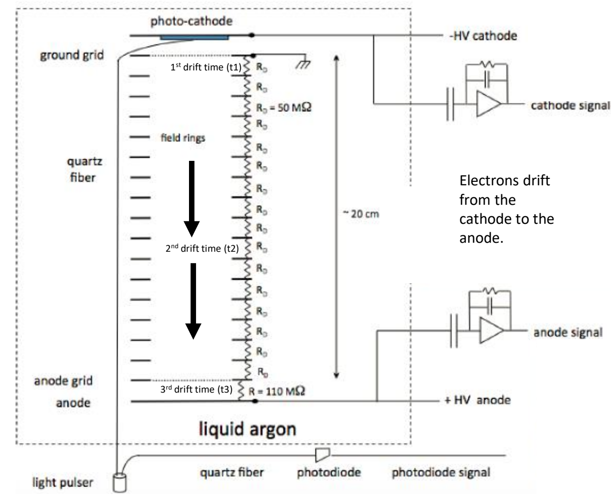

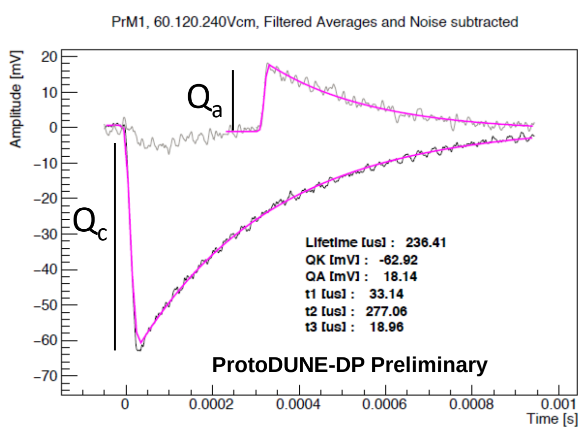

Obtaining a Drift Electron Lifetime

- Measure Q_a/Q_c, charge between cathode and anode.
  - $Q_a/Q_c=e^{-t/\tau}$
- Convert the ratio into a τ.
  - $\tau = \frac{1}{\log\left(\frac{Q_a}{Q_c}\right)}(t_{drift})$
  - For Dual-Phase: $t_{drift} = t2 + 0.5(t1 + t3)$

[1] S. Amerio, S. Amoruso, M. Antonello, P. Aprili, M. Armenante, F. Arneodo et al., Design, *Construction and Tests of the ICARUS T600 Detector, Nuclear Inst. Methd Section A* 527(*2004*) 329–410.

Installation and Placement

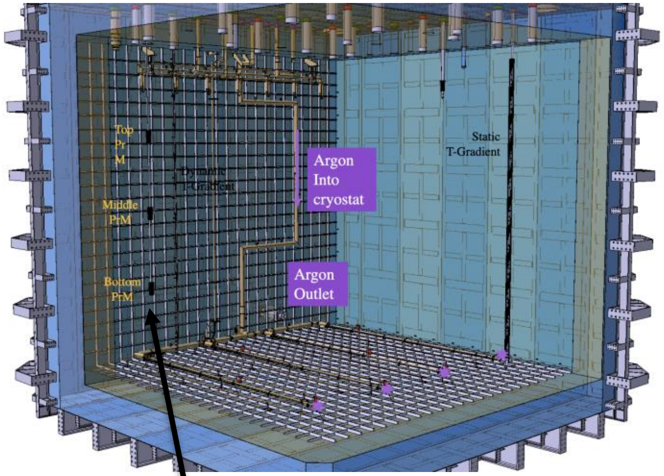

ProtoDUNE-SP

- Three purity monitors lie outside the TPC.
- ProtoDUNE-SP started operation in September 2018. Ceased operations on July 20th, 2020.

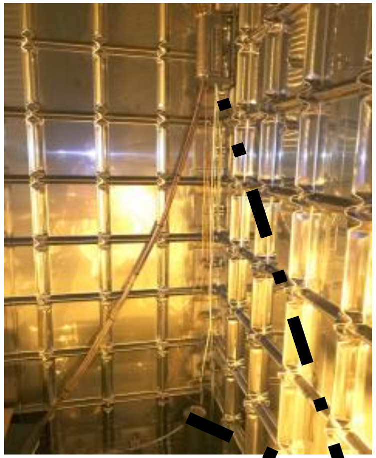

ProtoDUNE-DP

- Two short purity monitors of drift length around 20 cm sit up against a corner of the cryostat.
- One purity monitor of much longer drift length (not pictured) was also installed.
- Started operation in August of 2019. Currently taking cosmic data.

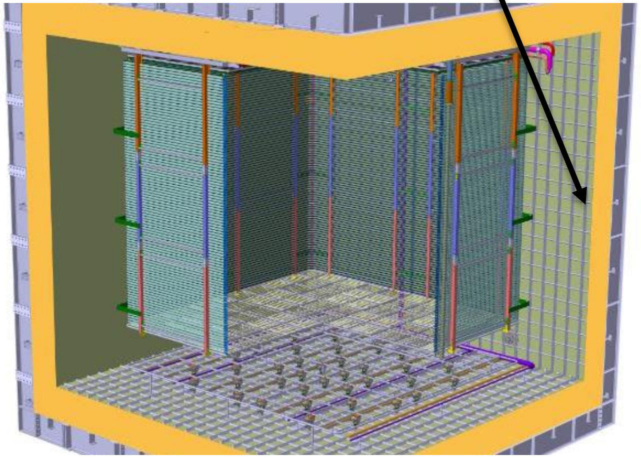

Performance of Purity Monitors

- **The DUNE Far Detector has a tech. req. that τ=3 ms and a tech. spec. that τ>10 ms for both detector technologies.**

ProtoDUNE-SP

Measured high purity throughout operations except for an incident in summer of 2019.

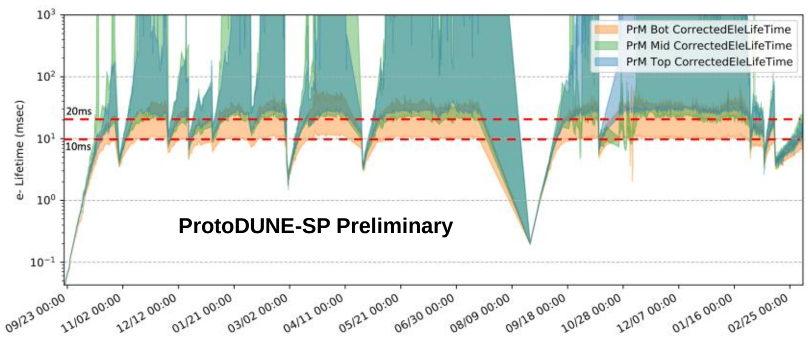

Dates start in 2018 and end in 2020.

The TPC drift electron lifetime was measured directly using cosmic muons to validate purity monitor measurements.

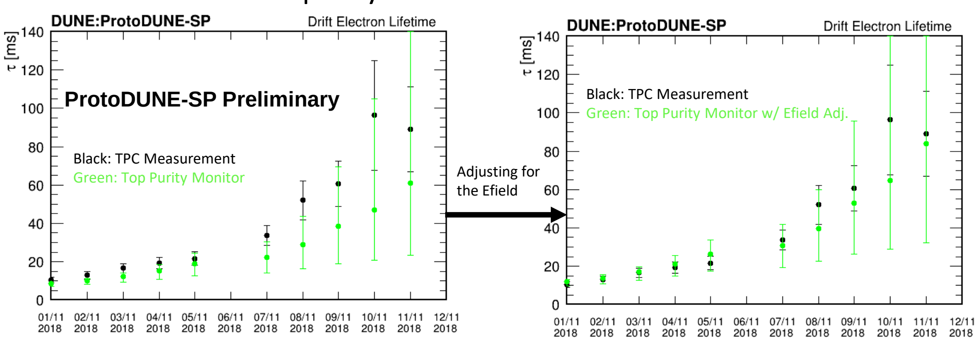

Attachment rates for impurities differ based on the electric field of the drift volume. The purity monitors operate at around 25 V/cm, while the TPC operates at 500 V/cm.

ProtoDUNE-DP

Purity has increased over the last year of operations and met DUNE Far Detector specifications.

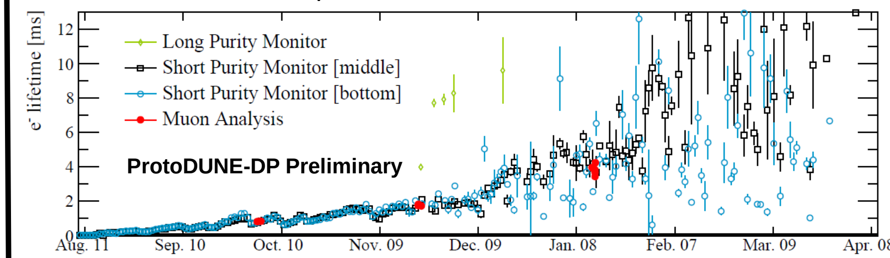

Dates start in 2019 and is still operating in 2020. ProtoDUNE-DP also included a purity monitor with a much longer drift length, referred to as the Long Purity Monitor.

Cosmic muon measurements of the drift electron lifetime agree with the purity monitors in ProtoDUNE-DP.

Conclusion

- ProtoDUNE uses the same design of purity monitors as the DUNE Far Detector will and its lessons will inform the operation at the Far Detector modules [2].
- Both prototype modules measured a drift electron lifetime that met DUNE Far Detector specifications.
- Purity monitor data is being utilized to calibrate datasets for precision dE/dx measurements for both detectors.

[2] B. Abi, A. A. Abud, R. Acciarri, M. Acero, G. Adamov, M. Adamowski et al., *First Results on ProtoDUNE-SP Liquid Argon Time Projection Chamber Performance from a Beam Test at the CERN Neutrino Platform*, *arXiv preprint arXiv:2007.06722*(2020) .

DEEP UNDERGROUND NEUTRINO EXPERIMENT

UNIVERSITY of HAWAIʻI MĀNOA

Moveable Thermometer System in ProtoDUNE

Ranjan Dharmapalan
for the DUNE Collaboration

ICHEP 2020 | PRAGUE

Moveable Thermometer System in ProtoDUNE

- The Deep Underground Neutrino Experiment (DUNE) will employ the largest Liquid Argon Time-Projection Chamber (LArTPC), to date, as its far detector.

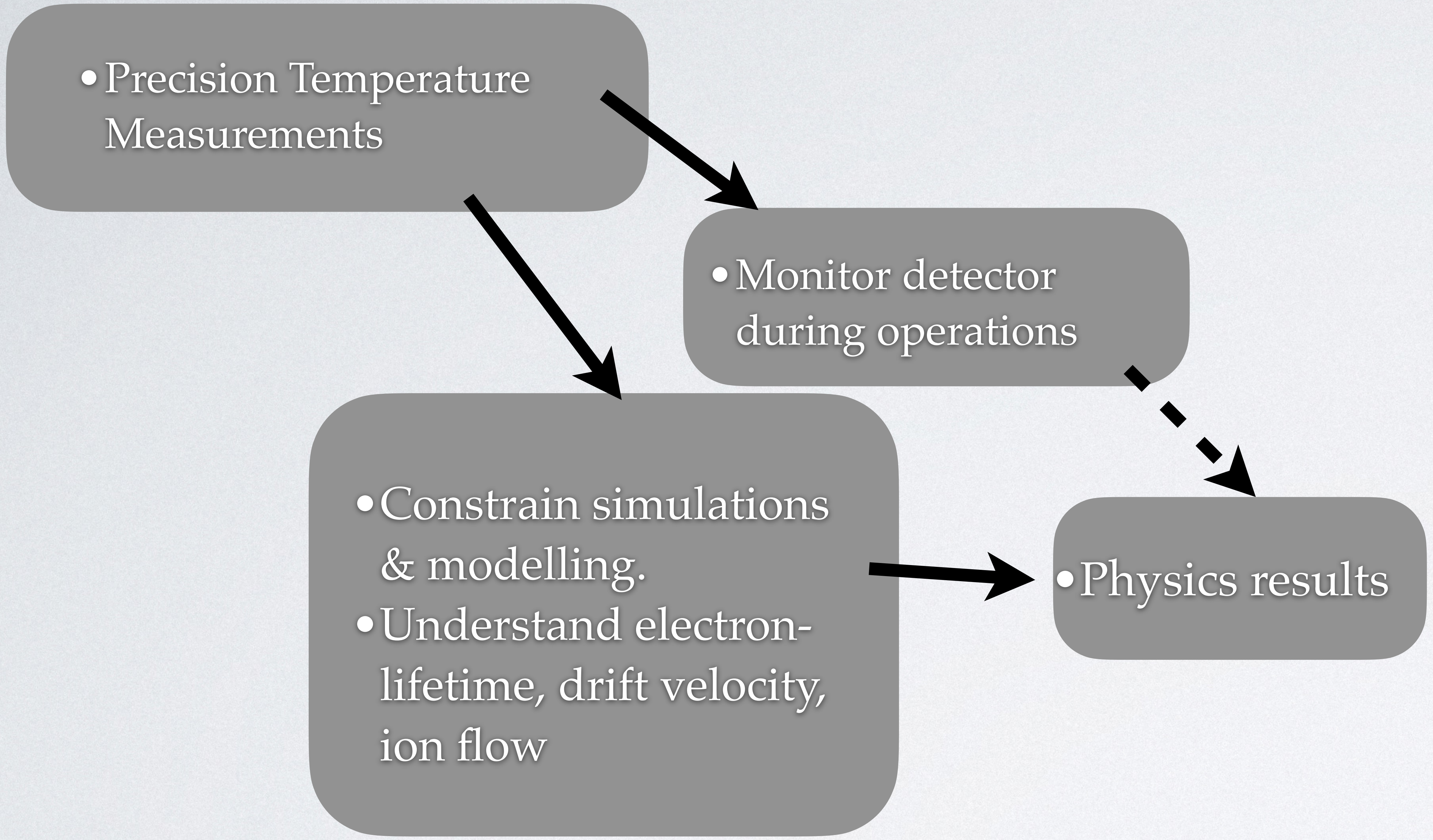

- Precise monitoring of the 17 kilo-ton (10 kilo-ton fiducial mass) liquid Argon temperature will be crucial to achieve the ultimate physics goals of the experiment.

- ProtoDUNE is a 0.7 kilo ton scale prototype at the CERN Neutrino Platform and a test-bed to evaluate technologies for the eventual DUNE experiment.

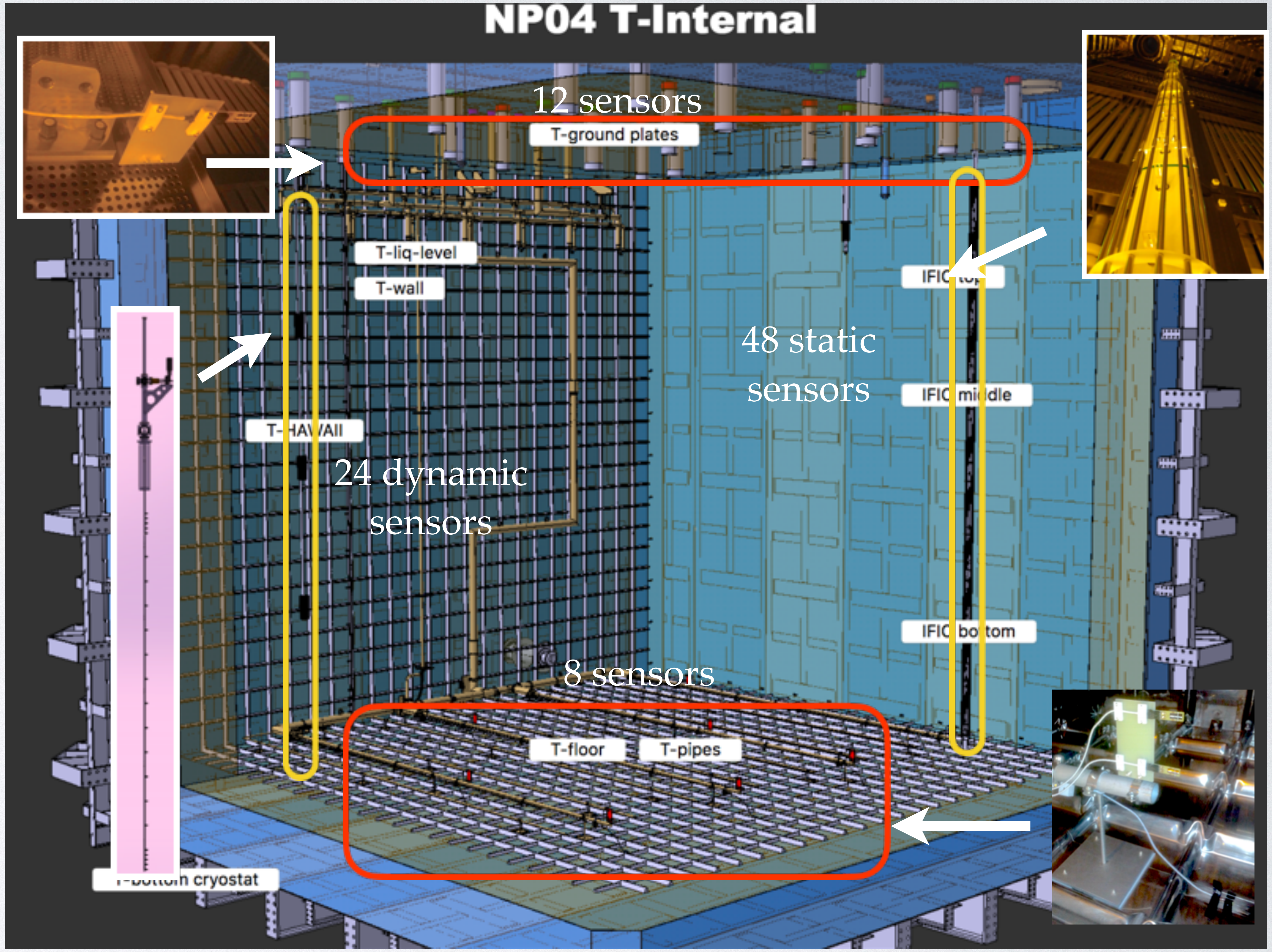

Schematic showing various temperature sensors and their location in the ProtoDUNE cryostat. The dynamic temperature profiler is shown on the left.

Moveable Thermometer System in ProtoDUNE

- The dynamic temperature profiler is a 7.5 meter moveable vertical array of 24 sensors, capable of measuring cryogenic temperatures with a precision of few milli kelvin.

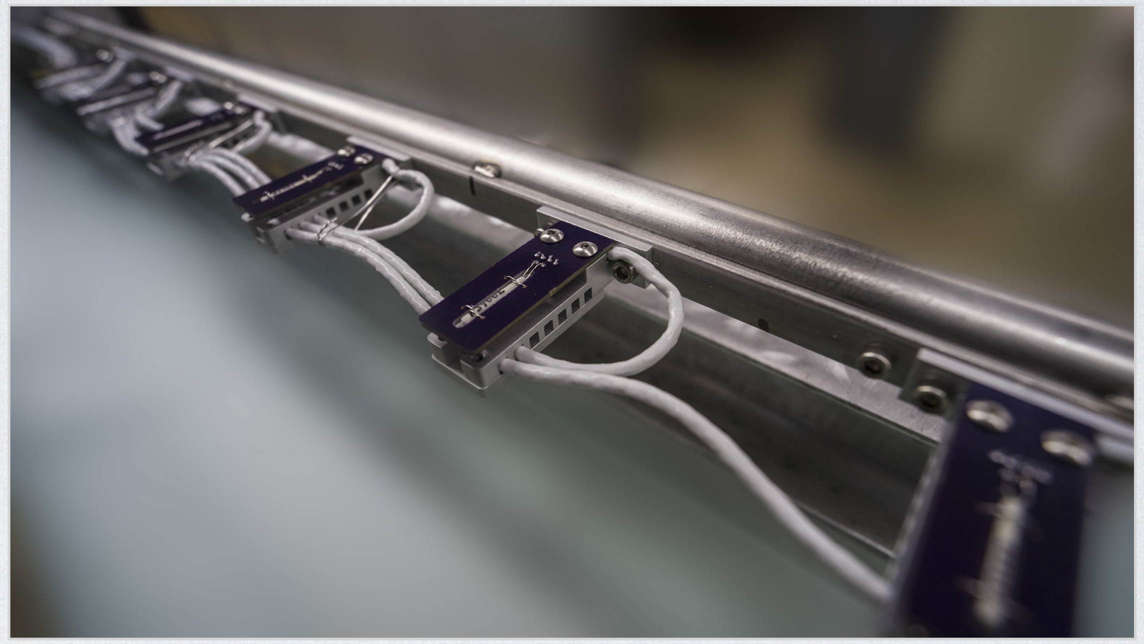

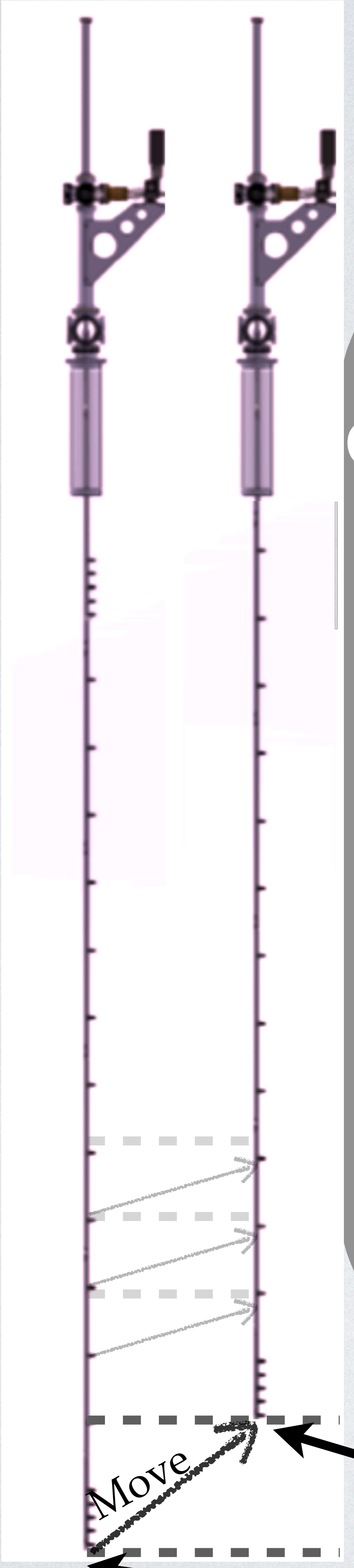

- In the schematic on left:

$\text{Offset}_{(\text{Sensor6})} = T_{(\text{Sensor6})} - T_{(\text{Sensor1 @ location of Sensor6})}$

- Mechanical constraints limit the number of moves and some locations are probed by multiple sensors.
- Given a certain number of moves, sensors, and temperatures we can extrapolate using a χ^2 minimization technique:

$$\chi^2 = (S_1 - T_1) + (S_2 - \text{offset}_2 - T_1) + (S_1 - T_2)$$
$$\ldots + (S_n - \text{offset}_n - T_{(n-1)})\ldots$$

Sensor1 @ location of sensor 6

Sensor1 @ location 1

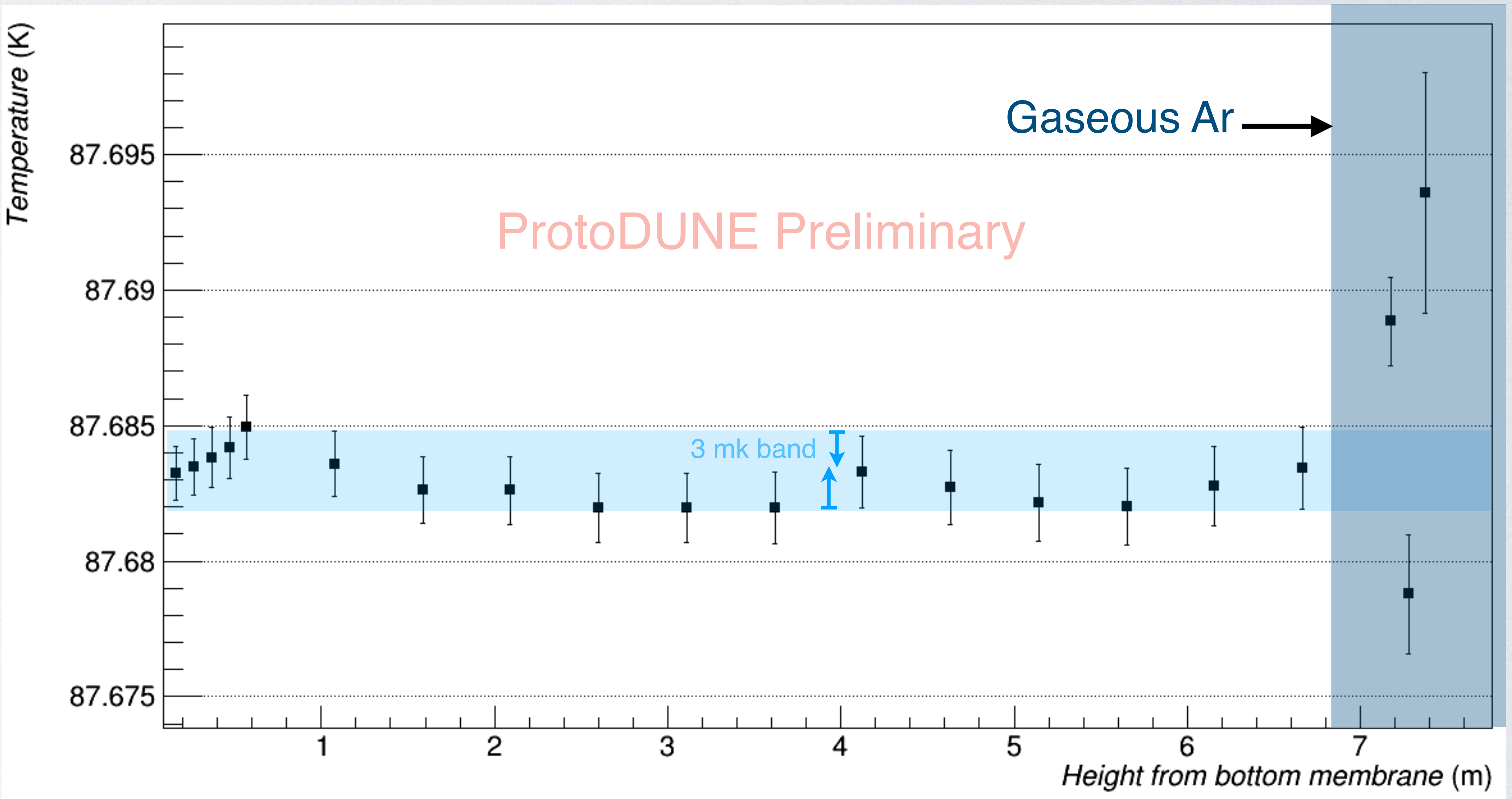

- Including the offsets corrects for residual parasitic resistance and electromagnetic noise and yields a relative accuracy of 2-3mK.

Moveable Thermometer System in ProtoDUNE

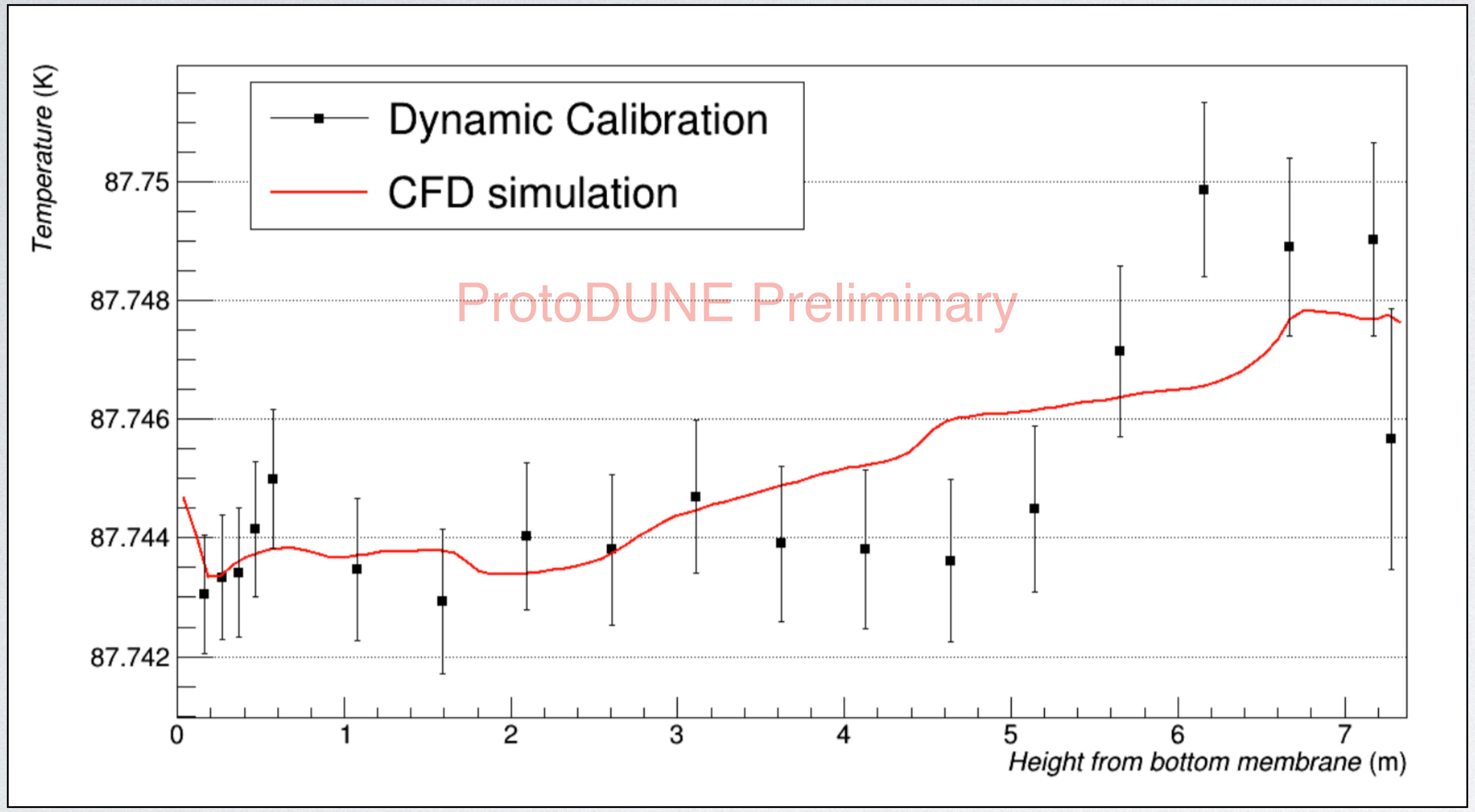

- The ability to move the sensors vertically is utilized to cross-calibrate the static sensors. The sensor values are then used to validate Computational Fluid Dynamic (CFD) models of liquid Argon in the detector.

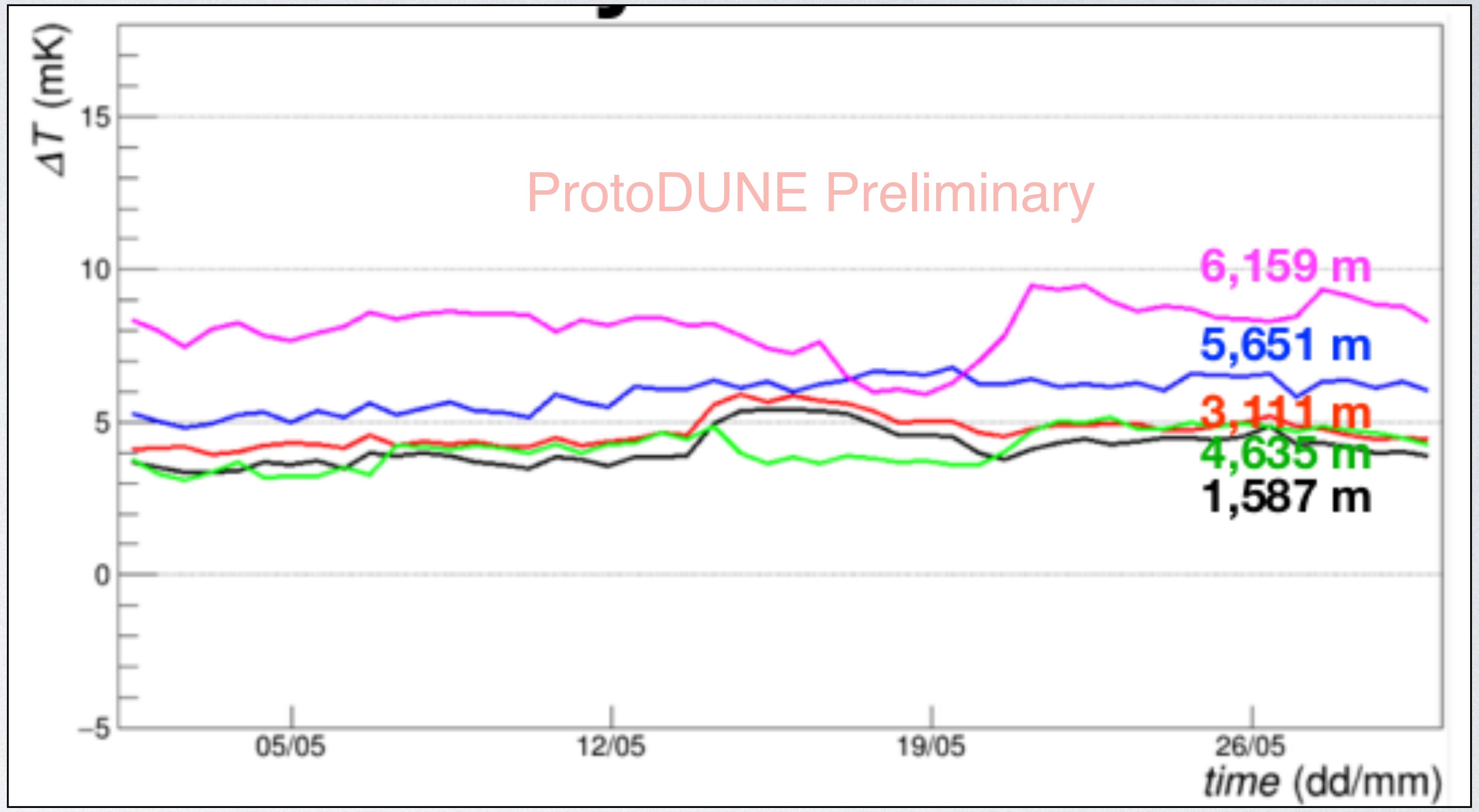

- Stability of the dynamic temperature profiler over two months is shown below. Here ΔT is the difference between the bottom-most sensor and the sensor at the heights shown.

Conclusions:

- The dynamic temperature profiler was continuously operating in ProtoDUNE since fall 2018. The system has been stable and exhibited no fatigue in cryogenic operation.
- The system has an outstanding accuracy of around 2 to 3 mk.

Improved Limits on Sterile Neutrino Mixing from a Joint Search of the MINOS, MINOS+, Daya Bay, and Bugey-3 Experiments

Zhuojun Hu (Sun Yat-sen University)
On behalf of the Daya Bay and MINOS/MINOS+ Collaborations

- Neutrino oscillation
  - A neutrino created with a certain leptonic flavor can be found later to hold a different flavor.
  - Three neutrino weak states consist of superpositions of three mass states.
- Sterile neutrinos
  - Additional neutrino states that do not participate in any of the interactions in the Standard Model.
  - A fourth neutrino state may explain the anomalous excess observed by the Liquid Scintillator Neutrino Detector (LSND) and MinoBooNE experiments.

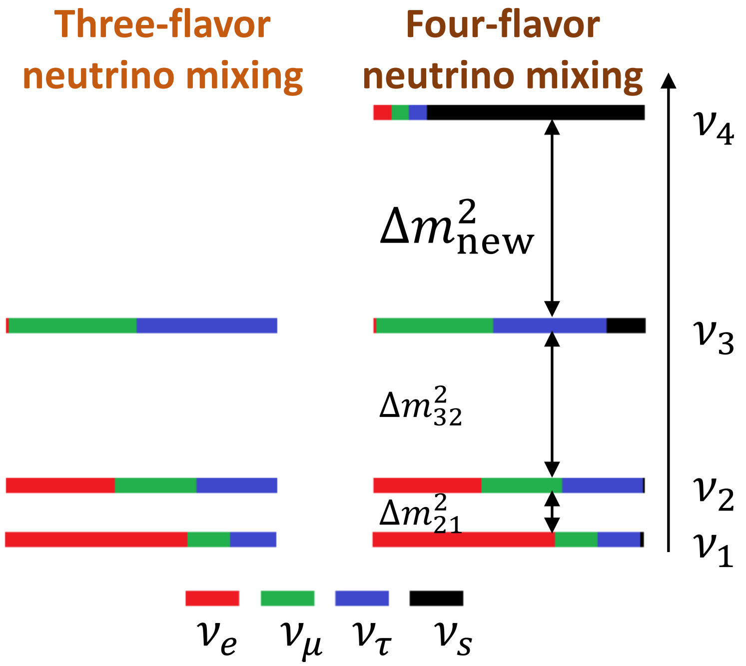

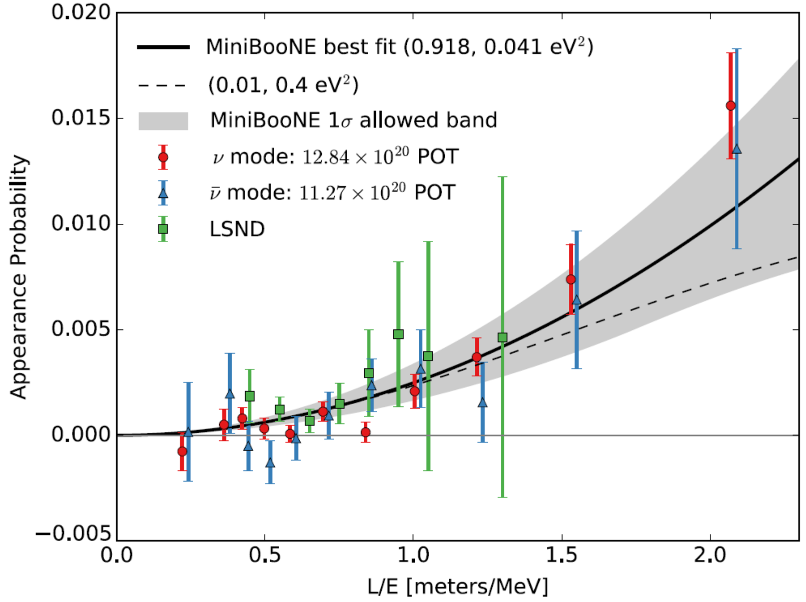

Significant excess by LSND and MiniBooNE: *Phys. Rev. Lett.* **121**, 221801 (2018).

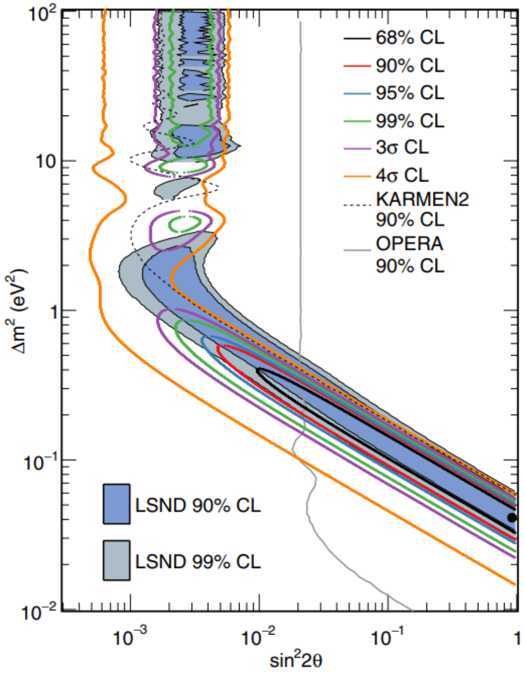

MiniBooNE allowed regions and LSND allowed regions: *Phys. Rev. Lett.* **121**, 221801 (2018).

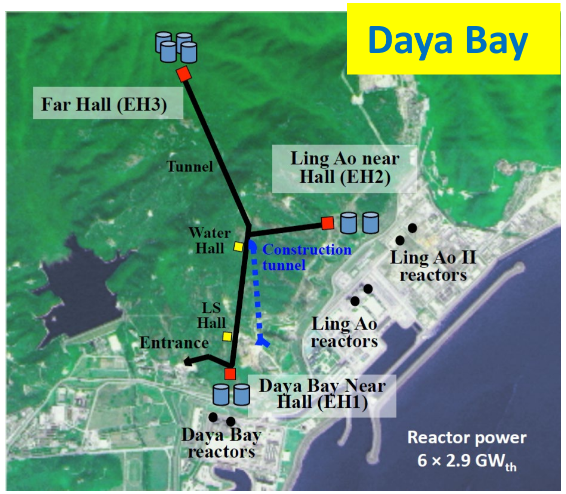

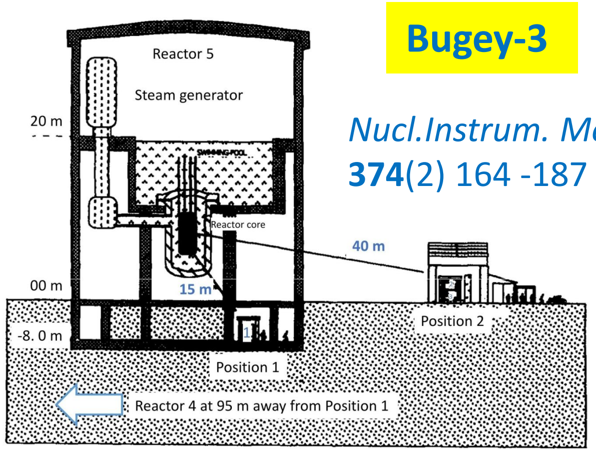

Nucl.Instrum. Meth. A **374**(2) 164 -187 (1996)

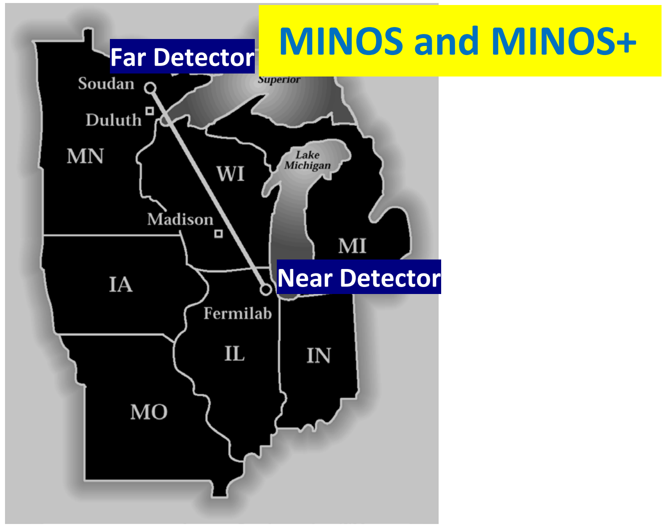

- reactor antineutrino disappearance.
- baselines. (~300 m - ~2000 m)

- reactor antineutrino disappearance.
- baselines. (15 m, 45 m, 90 m)

- accelerator neutrino disappearance.
- baselines. (ND 1 km, FD 735 km)

In presence of one sterile neutrino state, oscillation effects would appear in **disappearance** measurements as additional rate deficit and spectral distortion.

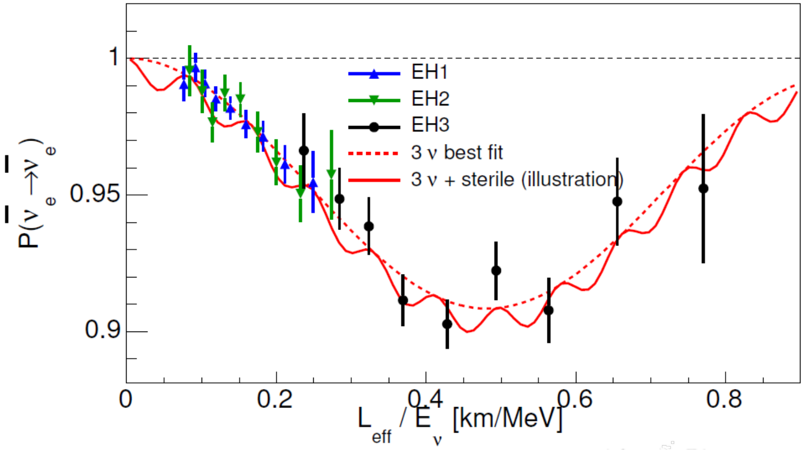

*additional spectral distortion expected with sterile neutrino oscillations at Daya Bay

$\bar{\nu}_e$ disappearance (reactor)

$$P_{\bar{\nu}_e \to \bar{\nu}_e} \approx 1 - \sin^2 2\theta_{13} \sin^2 \frac{\Delta m^2_{31} L}{4E} - \sin^2 2\theta_{14} \sin^2 \frac{\Delta m^2_{41} L}{4E}$$

$\nu_\mu(\bar{\nu}_\mu)$ disappearance (accelerator)

$$P_{\nu_\mu \to \nu_\mu} \approx 1 - \sin^2 2\theta_{23} \cos 2\theta_{24} \sin^2 \frac{\Delta m^2_{31} L}{4E} - \sin^2 2\theta_{24} \sin^2 \frac{\Delta m^2_{41} L}{4E}$$

Combination of two disappearance channels can constrain

The LSND and MinoBooNE **appearance** probability

$$P^{SBL}_{\overset{(-)}{\nu}_\mu \to \overset{(-)}{\nu}_e} = \sin^2 2\theta_{\mu e} \sin^2 \frac{\Delta m^2_{41} L}{4E}, \text{ where } \sin^2 2\theta_{\mu e} \equiv \sin^2 2\theta_{14} \sin^2 \theta_{24}$$

- Assuming presence of a light sterile neutrino, searches for sterile neutrino mixing are performed using $\bar{\nu}_e$ and $\nu_\mu(\bar{\nu}_\mu)$ disappearance, respectively.

Daya Bay + Bugey-3

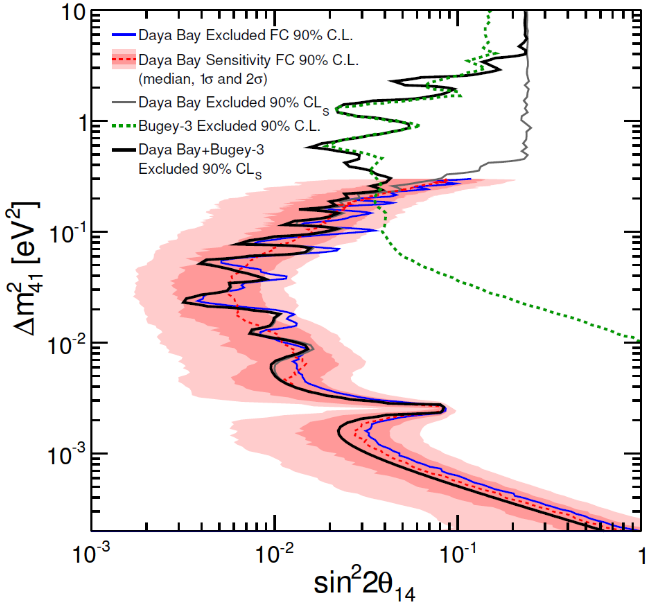

MINOS and MINOS+

Phys. Rev. Lett. **122**, 091803 (2019)

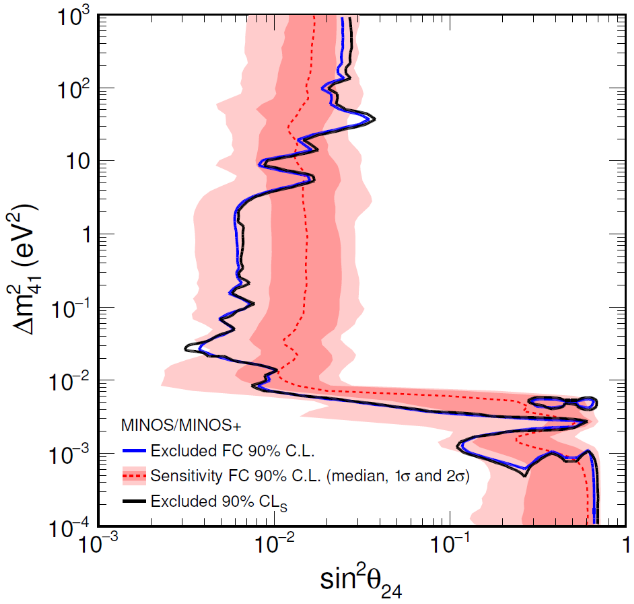

- Both are worlding-leading limits on sterile neutrino mixing.
- The disappearance measurements are combined using CL_s method.

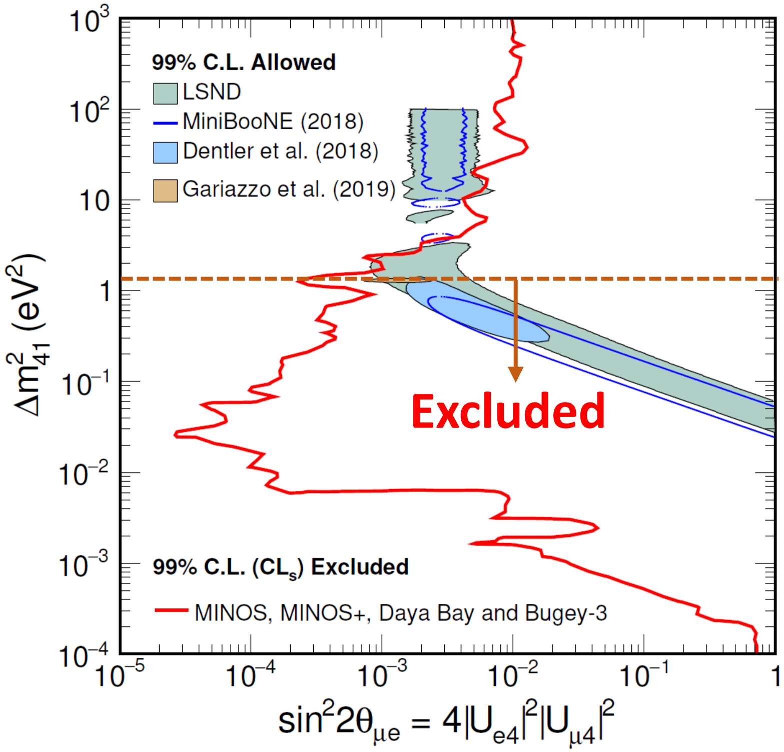

PRL accepted

Global fits:
Dentler et al. *JHEP* **08**, 010 (2018)
Gariazzo et al. *Phys. Lett. B.* **782**, 13 (2018)

- Tension between the $\overset{(-)}{\nu}_e$ appearance indications and the null results from disappearance channels is increased.
- We hope additional data from MINOS+ and Daya Bay can further quantify this tension in the future.

Thank you! Stay tuned

Measurement of $\sin^2 2\theta_{13}$ via neutron capture on hydrogen at Daya Bay

Jinjing Li
Mail: lijj16@mails.Tsinghua.edu.cn
Tsinghua university
On behalf of the Daya Bay Collaboration

IBD Selection and Backgrounds

- ❑ Next to 6 × 2.9 GW_{th} reactors providing large flux of $\bar{\nu}_e$
- ❑ 8 identical-design antineutrino detectors (ADs) deployed in three sites
- ❑ Inverse Beta Decay (IBD): $\bar{\nu}_e + p \rightarrow e^+ + n$
  - ❑ Prompt signal: kinetic energy of e^+ and annihilation gammas
  - ❑ Delayed signal: neutron capture gamma

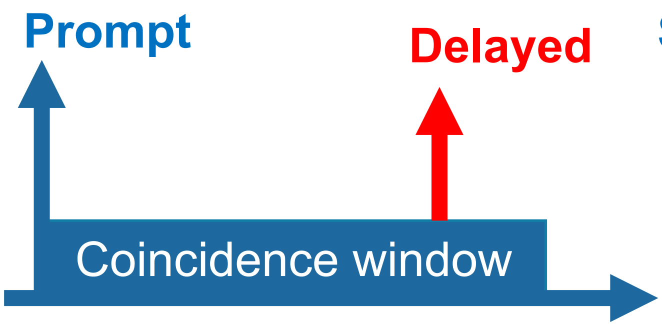

Select IBD with neutron captured on hydrogen (nH)

- ❑ Flasher cut & Muon Veto
- ❑ Energy cut: 1.5 MeV< E_p < 12 MeV, μ - 3σ < E_d < μ + 3σ
- ❑ Coincidence time: [1, 400] us
- ❑ Coincidence distance: [0, 500] mm
- ❑ Multiplicity cut: reject ≥ 3 coincidence

Correlated backgrounds:

- ❑ Muon-induced ^9Li/ ^8He:
- ❑ Muon-induced fast-neutron:
- ❑ Am-C calibration source

Accidental background:

- ❑ two uncorrelated AD events that satisfied the IBD selection criteria

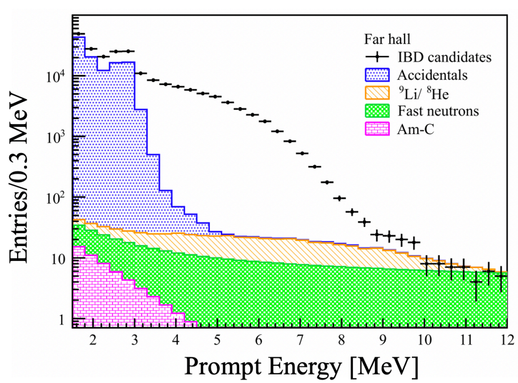

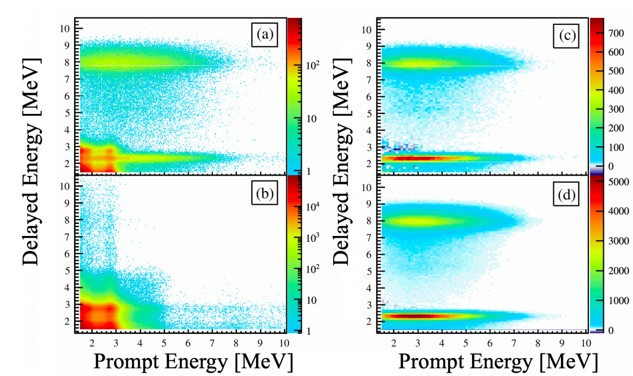

F.P. An et al, Phys. Rev. D 93 (2016) 072011

Efficiencies and AD Identicalness

- ❑ Studies with data
  - ❑ Distance cut
  - ❑ Coincidence time cut
  - ❑ Delayed energy cut
  - ❑ AD-uncorrelated uncertainty were estimated by comparison among 8 ADs.
- ❑ Studies with MC
  - ❑ Prompt energy cut, of which the uncertainty is fully due to the energy-scale variation among 8 ADs.

	Uncertainty (%)
Target protons ($N_{p,\mathrm{GdLS}}$)	0.03
Target protons ($N_{p,\mathrm{LS}}$)	0.13
Target protons ($N_{p,\mathrm{acrylic}}$)	0.50
Prompt energy (ε_{E_p})	0.10
Coincidence time (ε_T)	0.14
Delayed energy (ε_{E_d})	0.35
Coincidence distance (ε_D)	0.40
Combined (N_ε)	0.57

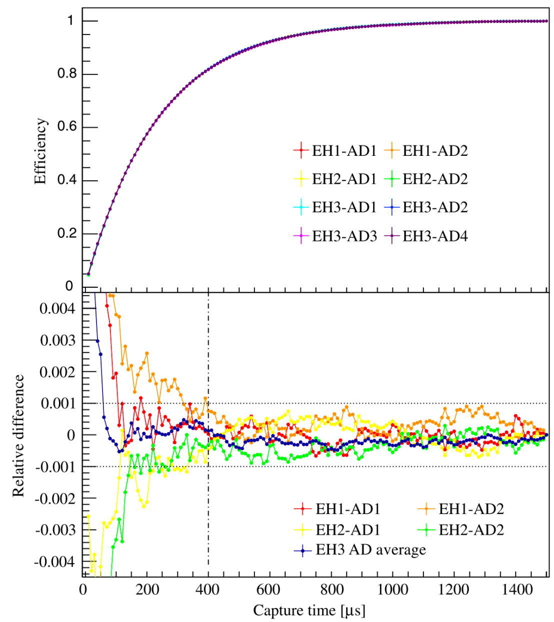

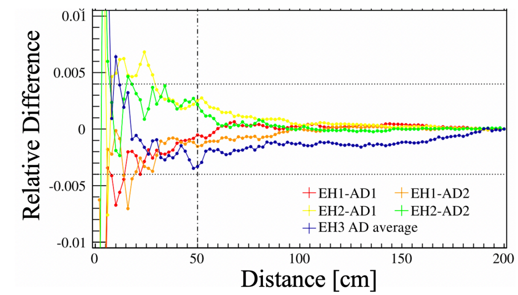

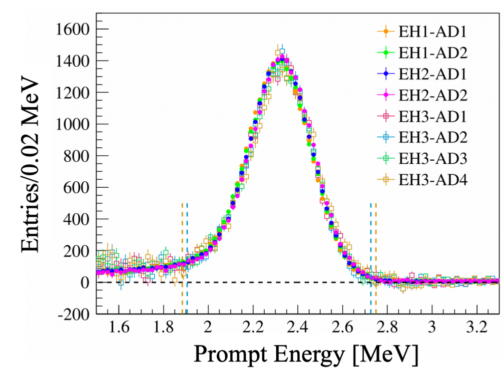

- ❑ Other IBD selection cuts have negligible uncertainty, such as: multiplicity cut, muon veto, etc.
- ❑ In our last publication, the uncertainty of distance cut and delayed energy cut are dominated in final analysis. New analysis is expected to yield a significant improvement.

F.P. An et al, Phys. Rev. D 93 (2016) 072011

Oscillation Analysis Result

➢ χ^2 function of the rate-only analysis

$$\chi^2 = \sum_{\text{detector}} \frac{\text{Measurement} - \text{Prediction} \times (1 + \varepsilon_{\text{reactor}} + \varepsilon_{\text{efficiency}}) - \text{Background} \times (1 + \varepsilon_{\text{bkg}})}{\sqrt{\text{Measurement}}} + \text{pull terms}$$

- ❑ Using 621 days of data, and ~1.0 million antineutrino interactions, we measured that $\sin^2 2\theta_{13} = 0.071 \pm 0.011$.
- ❑ Right figure: Measured IBD rate vs. time for each experimental hall (blue points). Each point spans one week.

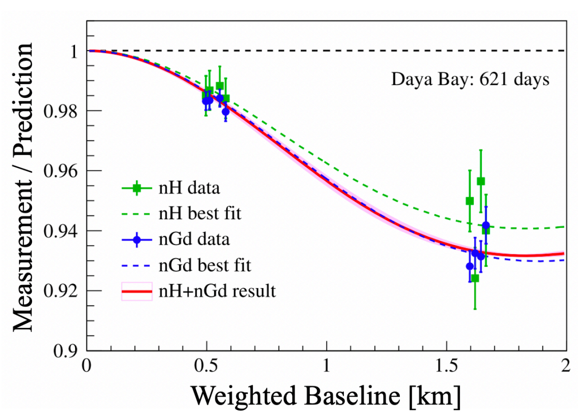

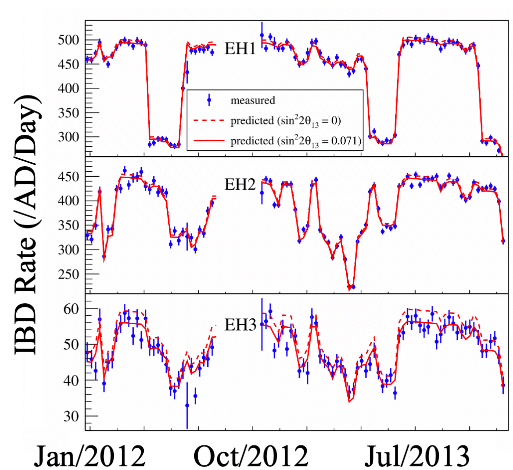

➢ Towards a Rate & Spectral Shape Measurement

- ❑ Deficit of IBD rate at different neutrino energy range
- ❑ Good understanding of detector energy response

Thank you! Stay tuned~

F.P. An et al, Phys. Rev. D 93 (2016) 072011

Study of Fuel Evolution and Isotope Contribution Decomposition at Daya Bay

Wei Wang *(on behalf of the Daya Bay Collaboration)*

Sun Yat-sen University

ICHEP 2020, Prague, Czech

- *Reactor antineutrino anomaly and its spectrum discrepancy*
- *Reactor fuel evolution analysis and IBD yield measurements*
- *Flux and spectral decomposition analyses*

Reactor Antineutrino Anomaly and the Spectrum Discrepancy

- Reactor Antineutrino Anomaly (RAA) has been haunting the community since 2011
- So has been the reactor antineutrino spectrum discrepancy since 2014.

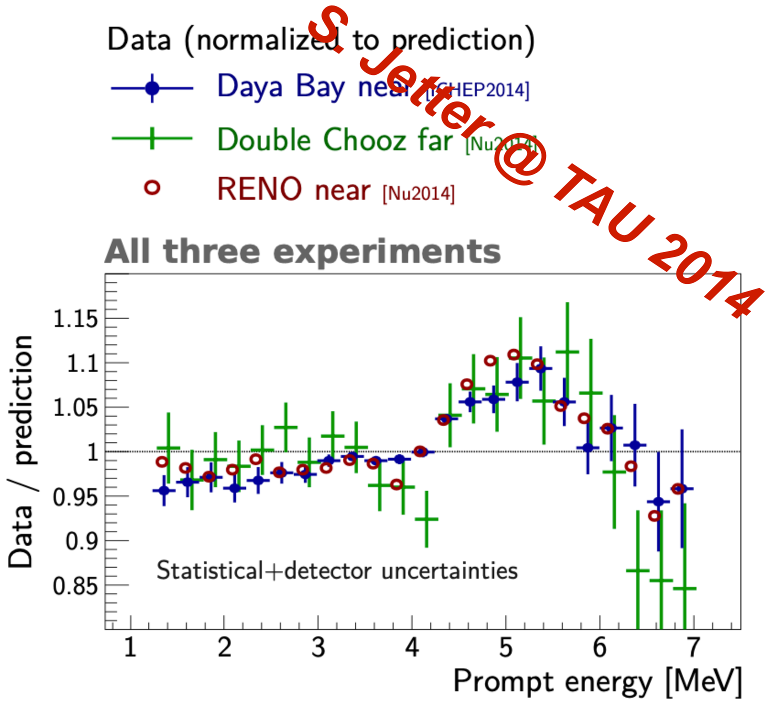

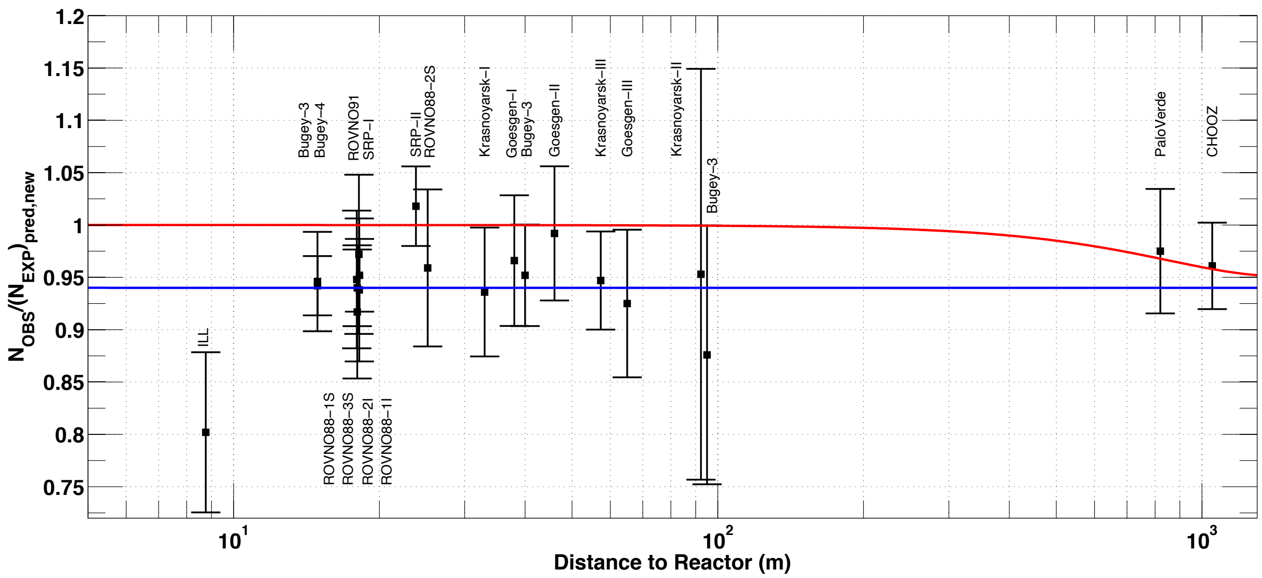

- Revaluation of ILL beta spectra data
- Combined with *ab initio* approach

➡ ~6% deficit

Daya Bay RAA Results and Correlation with Isotopes

- An effective fission fractions can be evaluated based on the data passed from the power plant
- IBD yields can be evaluated or measured using the Huber-Mueller model or the Daya Bay data

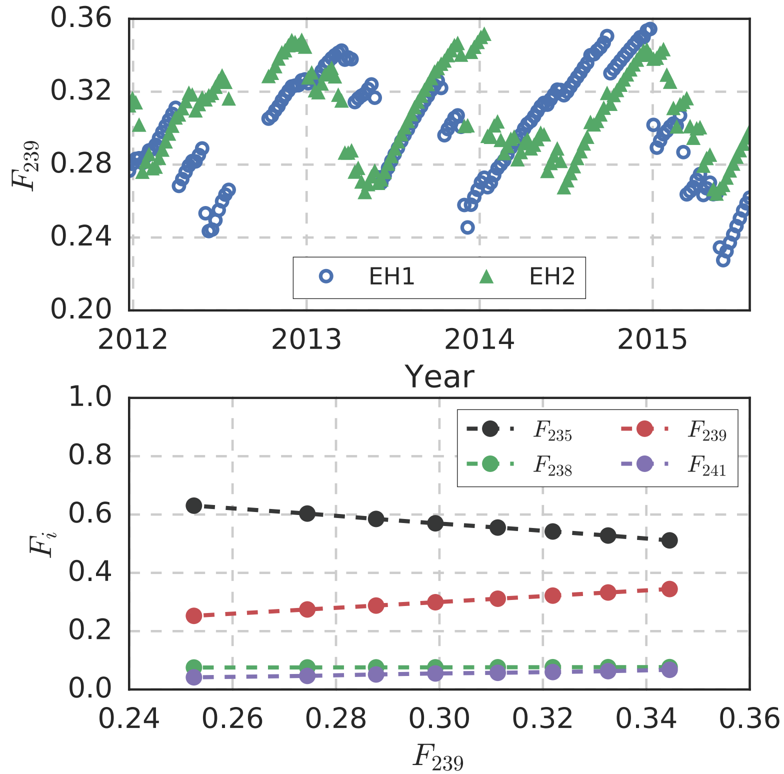

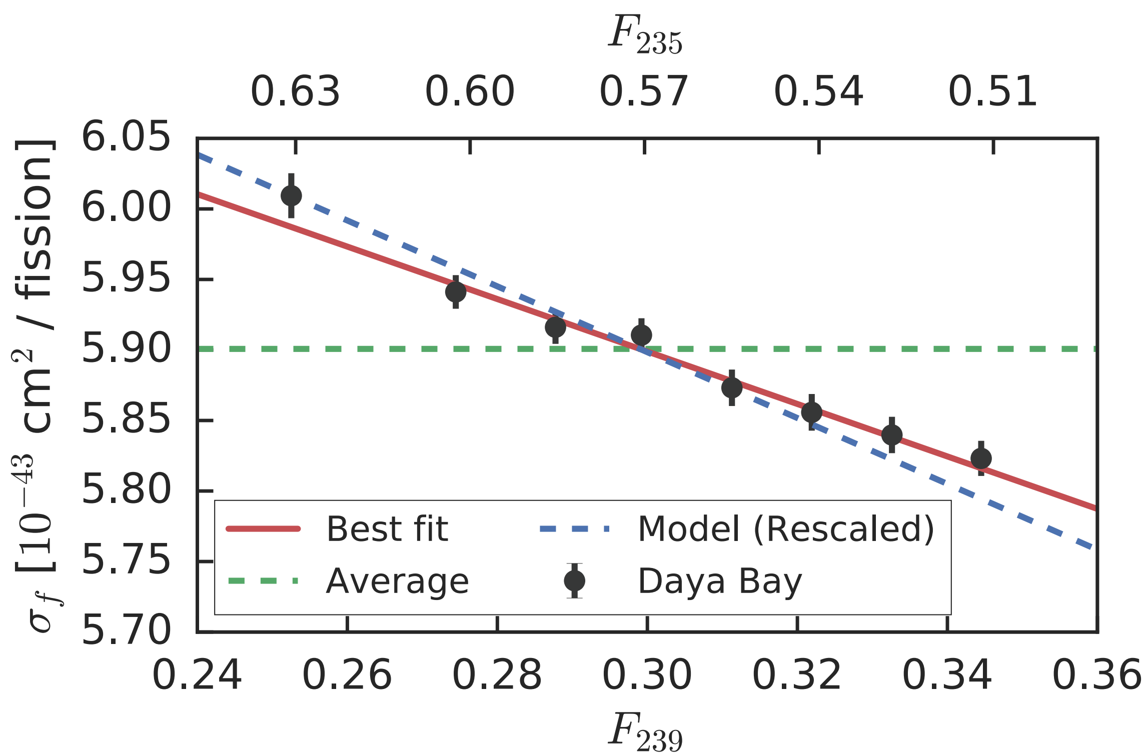

Decomposing Fission Isotope Contributions

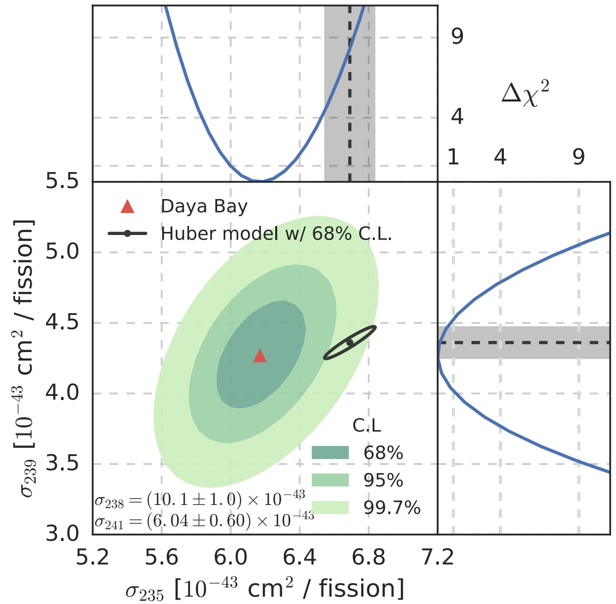

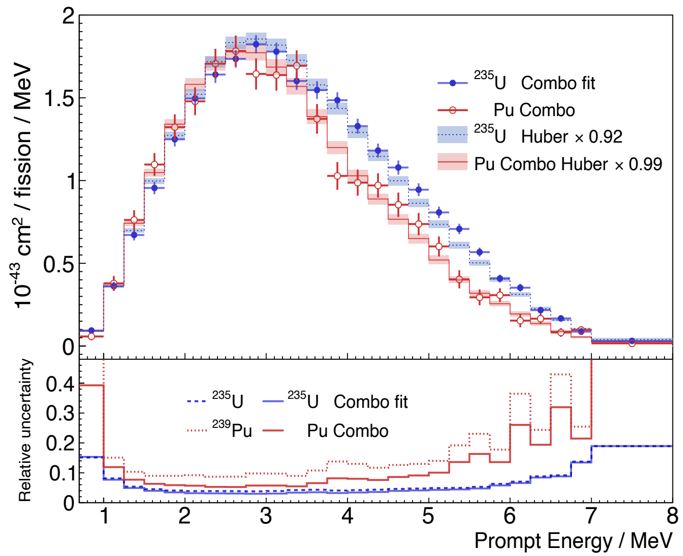

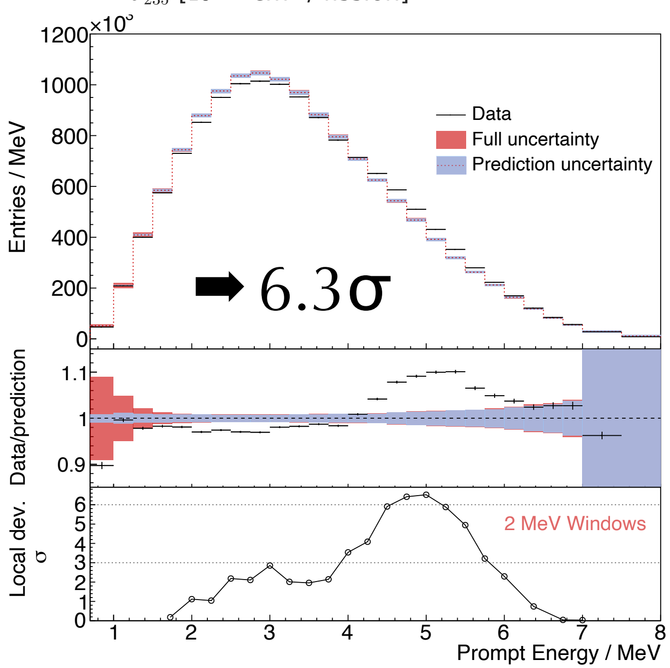

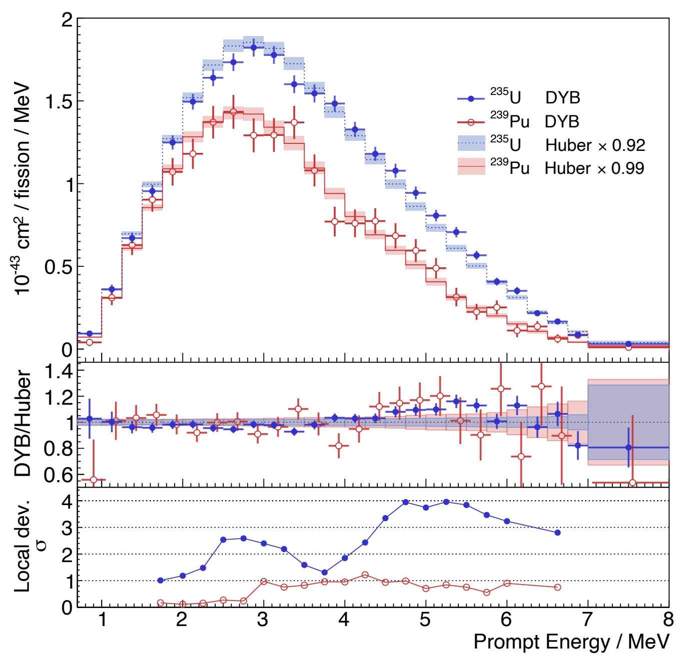

- With 1230 days of data, a correlation analysis shows that ^{235}U is more likely to be responsible RAA
- A spectral decomposition is carried out for the first time
- Spectral decomposition also shows that ^{235}U is responsible for the "bump", 4σ; while ^{239}Pu is consistent within 1.2σ

Reactor Antineutrino Flux and Spectrum Measurement at Daya Bay and Study of its High-Energy Component

Yuzi Yang
Tsinghua University
On behalf of Daya Bay Collaboration

ICHEP 2020 | PRAGUE

Daya Bay Experiment

- Six commercial reactors
  - Thermal power of each reactor is 2.9 GW (~2x10^{20} $\bar{\nu}_e$/s/GW)

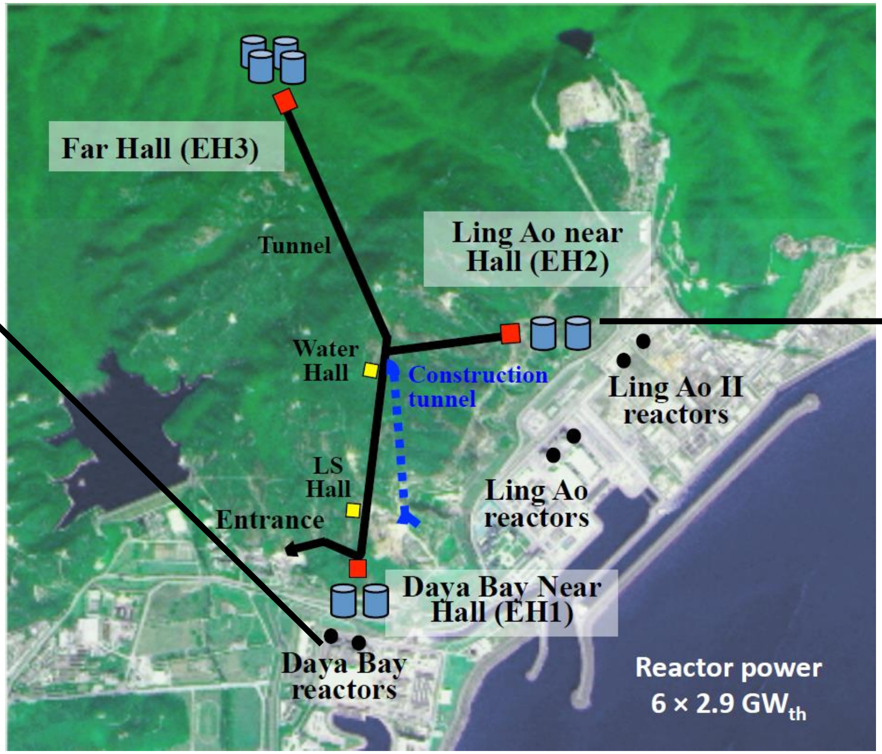

- Eight antineutrino detector (ADs) in three experimental halls (EHs)

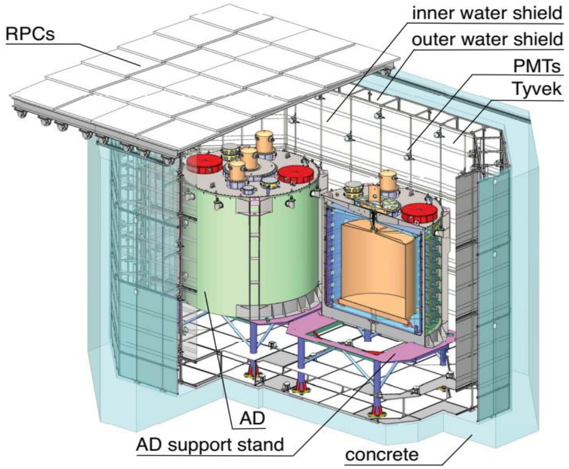

- Antineutrino is detected via inverse beta decay process:

$$\overline{\nu}_e + p \rightarrow e^+ + n$$

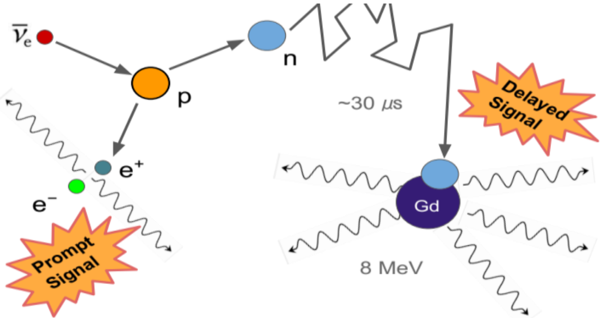

Improvement of uncertainty

- The dominant uncertainty on the neutron detection efficiency is reduced by 56%.

source	Previous value	Previous rel. err.	This work value	This work rel. err.
statistic	-	0.1%	-	0.1%
oscillation	-	0.1%	-	0.1%
target proton	-	0.92%	-	0.92%
reactor				
power	-	0.5%	-	0.5%
energy/fission	-	0.2%	-	0.2%
IBD cross section	-	0.12%	-	0.12%
fission fraction	-	0.6%	-	0.6%
spent fuel	-	0.3%	-	0.3%
non-equilibrium	-	0.2%	-	0.2%
ε_{IBD}				
ε_n	81.83%	1.69%	81.48%	0.74%
ε_{other}	98.49%	0.16%	98.49%	0.16%
total	-	2.1%	-	1.5%

F. P. An et al. Phys. Rev. D 100 (2019) 052004

- FADC data and new calibration campaign in 2017 help to reduced the energy nonlinearity uncertainty.

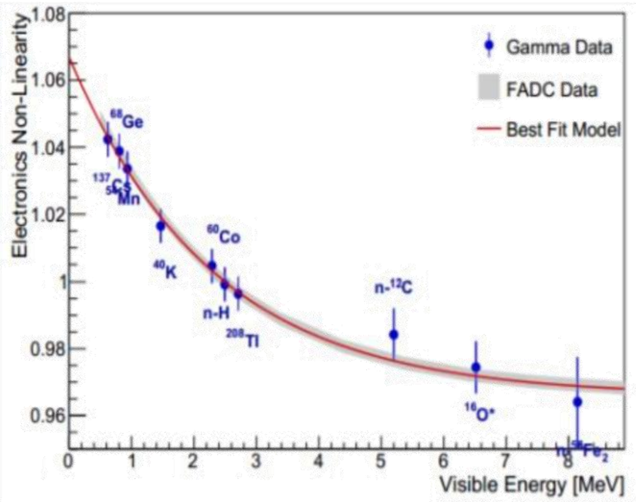

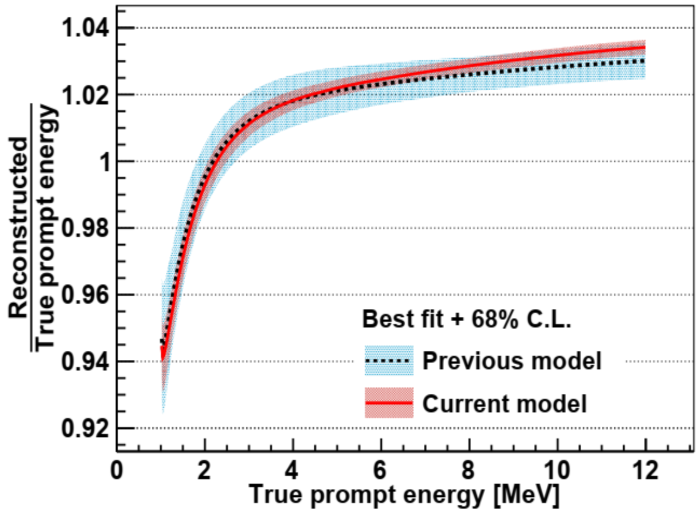

- Uncertainties in the absolute energy calibration is reduced to less than 0.5% from previous 1.0% for visible energies larger than 2MeV.

F. P. An et al. Phys. Rev. Lett 121 (2018) 241805

Antineutrino flux and spectrum measurement

- Using 1230 days of data, the new reactor antineutrino flux measurement at Daya Bay is: $\sigma_f = (5.91 \pm 0.09) \times 10^{-43} cm^2/fisson$
- The ratio of data and prediction is:

$$R = 0.952 \pm 0.014(exp) \pm 0.023(model)$$

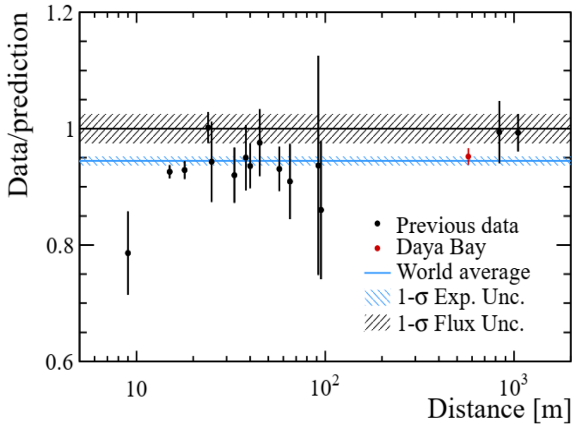

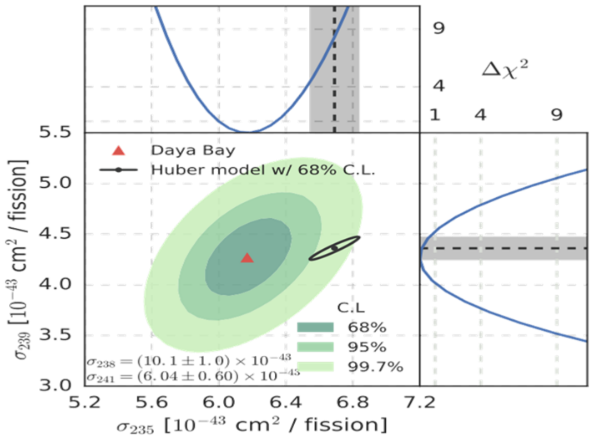

F. P. An et al. Phys. Rev. Lett 121 (2018) 241805
F. P. An et al. Phys. Rev. Lett 118 (2017) 251801

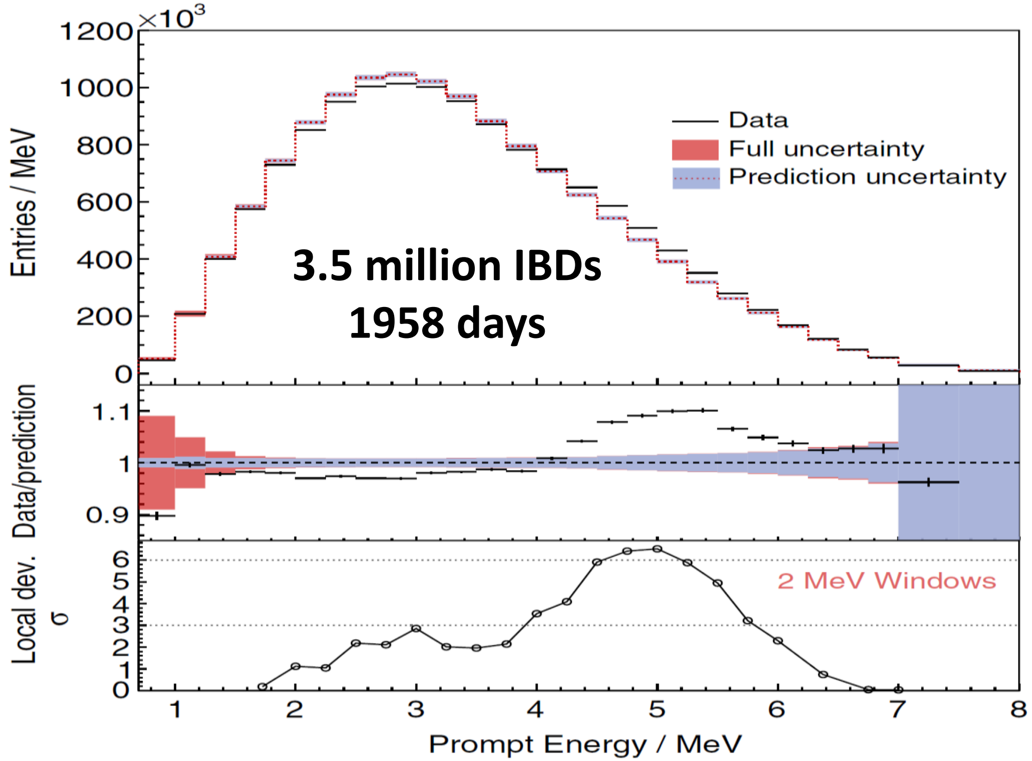

- A bump is obvious in the energy range 4-6MeV.
- The spectral shape disagrees with the Huber-Mueller model at 5.2 σ from 0.7 to 8 MeV.

F. P. An et al. Phys. Rev. Lett 123 (2019) 111801

How many candidates from high-energy reactor antineutrino (HERA) at Daya Bay?

Energy and Vertex Reconstruction in JUNO

Guihong Huang for the JUNO collaboration

IHEP

Jul.30, 2020

40th International Conference on High Energy Physics

The JUNO experiment

- A multi-purpose observatory
  - Determine the neutrino mass ordering
  - Precisely measure $\sin^2 2\,\theta_{12}$, Δm^2_{21}, Δm^2_{31}
  - Study the solar neutrinos, supernova neutrinos, diffuse supernova neutrino background, etc.

- $3\%/\sqrt{E}$ unprecedented energy resolution
  - Total light level ~1200 pe / MeV
  - Attenuation length > 20 m @ 430 nm
  - Photocathode coverage ~75%
  - PMT detection efficiency > 27%

schematic view of JUNO detector

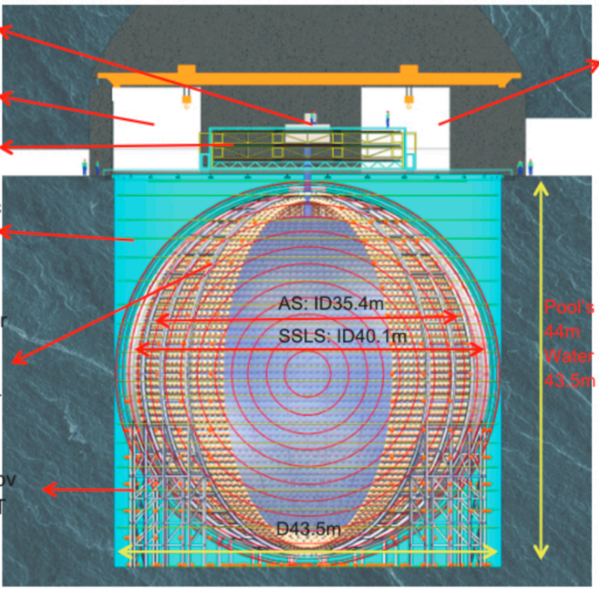

AS: Acrylic sphere; SSLS: stainless steel latticed shell

Charge and time combining maximum likelihood estimation

- The expected light level of PMTs $E * \mu_{i,0}(r, \theta, \theta_{pmt})$ **(3-D nPE map)**
- The pdfs of $t_r = t_h - t_f - t_d - t_0$ measured by PMTs $P_T(t_r|k, d)$
- The likelihood function

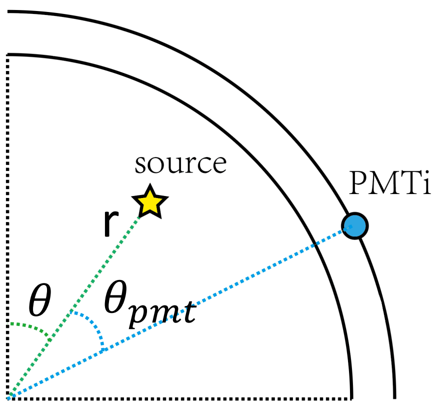

$$\mathcal{L}(\boldsymbol{q_1}, \boldsymbol{q_2}, \ldots, \boldsymbol{q_N}, \boldsymbol{t_{1,r}}, \boldsymbol{t_{2,r}}, \ldots, \boldsymbol{t_{N,r}}, \boldsymbol{k'_1}, \boldsymbol{k'_2}, \ldots, \boldsymbol{k'_N}|\vec{\boldsymbol{r}}, \boldsymbol{E}, \boldsymbol{t_0})$$
$$= \prod_{unhit} \boldsymbol{e}^{-\mu_j} \prod_{hit} \left[\left(\sum_{k=1}^{+\infty} \frac{\boldsymbol{e}^{-\mu_i} \boldsymbol{\mu_i^k}}{\boldsymbol{k}!} \boldsymbol{P_Q}(\boldsymbol{q_i}|\boldsymbol{k}) \right) \boldsymbol{P_T}\left(\boldsymbol{t_{i,r}}\middle|\boldsymbol{d_i}, \boldsymbol{k'_i}, \boldsymbol{t_0}\right) \right].$$

Performance, conclusion and outlook

- Most of the effects of the charge smearing, dark noise and vertex resolution on the energy resolution have been handled by QTMLE

- The impact of the dark noise, charge smearing and vertex resolution on the energy resolution need further studies.

$$Res.\ variation = 100 * \frac{R_{realistic} - R_{ideal}}{R_{ideal}}$$

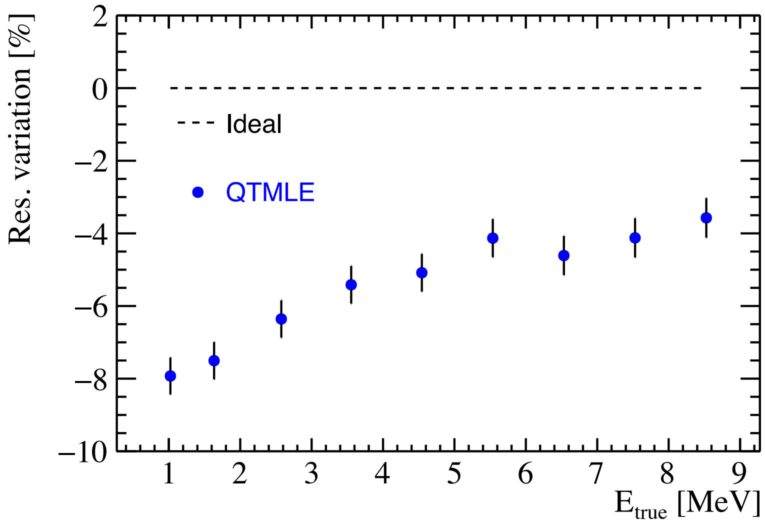

Status of the Veto System of JUNO

João Pedro Athayde Marcondes de André
for the JUNO Collaboration

IPHC/IN2P3/CNRS

July 30th, 2020

The JUNO Detector

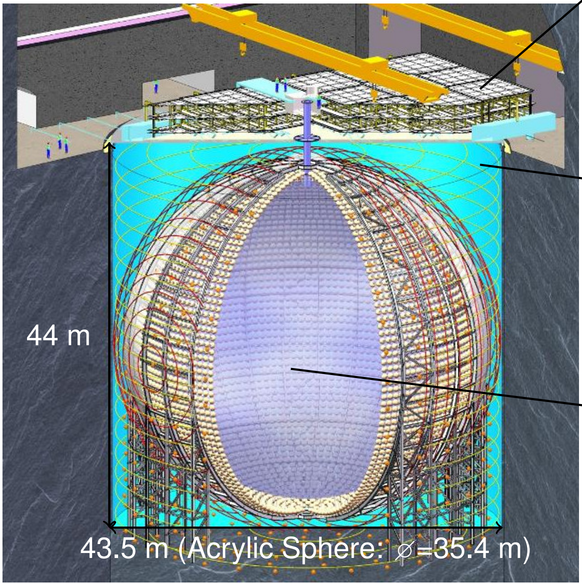

Top Tracker (TT)

- Precise μ tracker
- 3 layers of plastic scintillator
- $\sim$ 60% of area above WCD

Water Cherenkov Detector (WCD)

- 35 kton ultra-pure water
- 2.4k 20” PMTs
- High μ detection efficiency
- Protects CD from external radioactivity

Central Detector (CD) – $\bar{\nu}$ target

- Acrylic sphere with 20 kton liquid scint.
- 18k 20” PMTs + 26k 3” PMTs
- 3% energy resolution @ 1 MeV

Water Cherenkov Detector status

- Ultra pure water system:
  - Keep temperature and water quality
  - Start to install water pipes this year
  - 100 t/h system to be ready in 2021
- Bird cage: under production
- Liner:
  - Keep rock and water separate
  - Prevent Rn contamination from rock
  - Finishing installation tests
- Tyvek: same as Daya-Bay, prep. bidding
- Earth Mag. Field compensating coils:
  - reduce B on PMTs to $< 5\ \mu$T
  - ready for production
- PMT: use 2.4k of JUNO's 20" PMT
- All components ready or in production

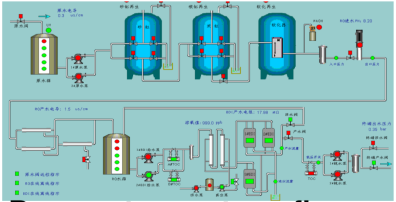

Pure water system, flow rate: ~100 t/h

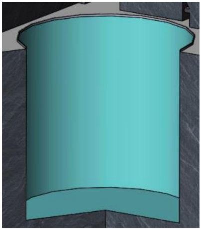

Pool liner

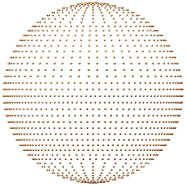

PMTs & Tyvek reflection film

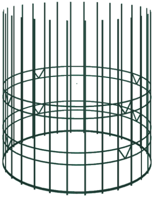

Bird cage &Tyvek reflection film

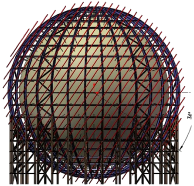

EMF coils

Top Tracker (TT) status

- TT refurbished from OPERA Target Tracker
  - Detector granularity $2.6 \times 2.6\ \text{cm}^2$ in X–Y
    - 0.2° median resolution for μ tracks
  - No aging of scintillator observed since OPERA
  - TT modules already delivered to JUNO site
  - Mechanical structure for TT re-designed
    - ready to start mass production
  - New electronics chain
    - FEB (w/ MAROC3): 1200 cards produced & tested
    - ROB: design being finalised, review in 2020
    - Concentrator (L1 trigger): testing prototype
    - L2 trigger card: design just started
- TT will be on time for JUNO

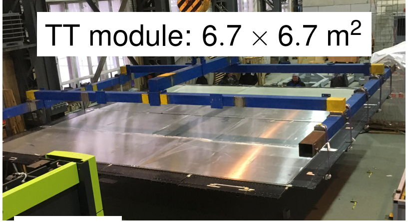

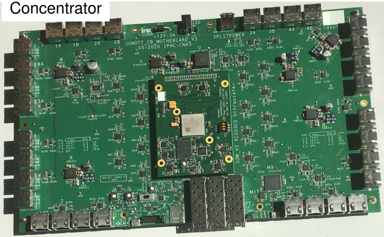

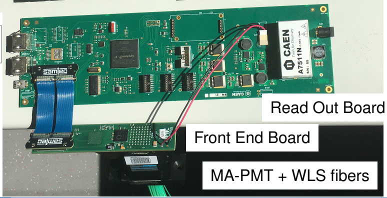

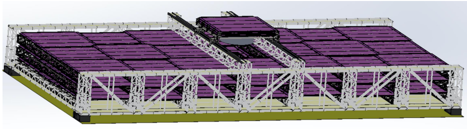

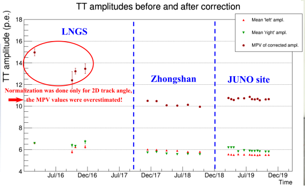

Poster:
The 3-inch Photomultiplier System of the JUNO experiment

Cécile Jollet (CENBG - CNRS/IN2P3) on behalf of JUNO collaboration
ICHEP 2020

JUNO detector design

- The experiment consists of a very large target made of 20 kton liquid scintillator detector.
- For 1 MeV, 1200 p.e. will be collected to ensure an energy resolution of 3%.

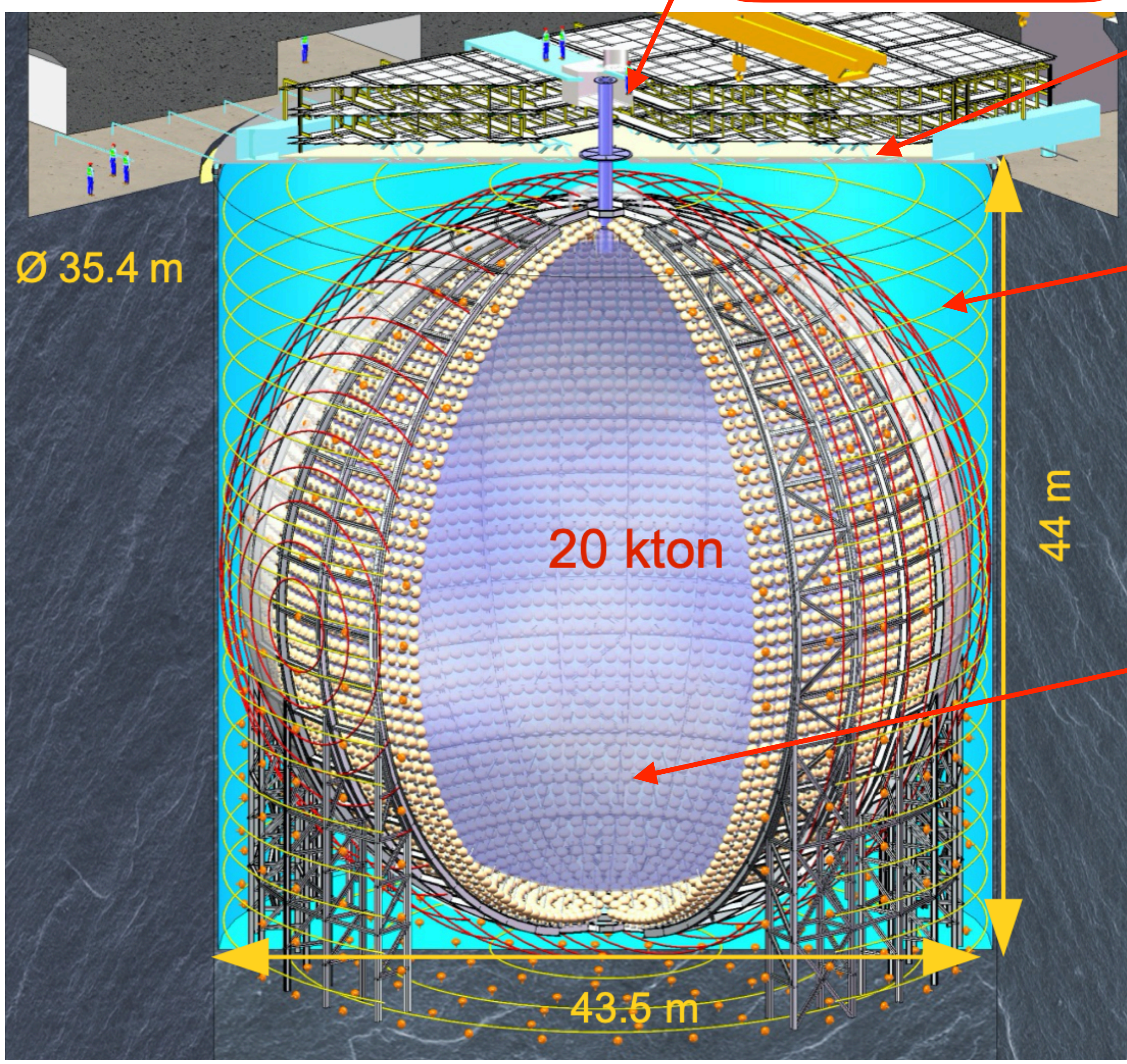

Calibration house
Multi-dimension calibration systems

Top Tracker
- Precise muon tracker
- 3 layers of plastic scintillator
- ~ 60% of area above WCD

Water Cherenkov Detector (WCD)
- 35 kton ultra-pure water
- 2400 20-inch PMTs
- High muon detection efficiency
- Protects CD against external radioactivity

Central Detector (CD) - Neutrino target
- Acrylic sphere with 20 kton liquid scintillator (LAB)
- 18000 20-inch PMTs and 25600 3-inch PMTs
- 3% energy resolution at 1 MeV.

The 3-inch PMT system

In addition to the 18,000 20-inch photomultipliers, 25,600 3-inch photomultipliers and their readout electronics will be deployed as a complementary photodetectors array in the Jiangmen Underground Neutrino Observatory.

- Complementary independent readout
- Precision calorimetry
- Improve inner-detector muon reconstruction resolution
- Improve particle discrimination
- Detection of neutron spallation
- Measurement of solar parameters
- Measurement of supernova high events rate

The 3-inch PMTs system